

Mechanistic Aspects of the Thermoreversible Gelation of Syndiotactic Poly(methyl methacrylate) in Toluene

K. Buyse and H. Berghmans*

Department of Chemistry, Katholieke Universiteit Leuven, Celestijnenlaan 200 F, B-3001 Leuven, Belgium

M. Bosco

POLY-tech S. Coop.r.l., AREA Science Park, Padriciano, 99, I-34012 Trieste, Italy

S. Paoletti

Department of Biochemistry, Biophysics and Macromolecular Chemistry, University of Trieste, via L. Giorgieri, 1 I-34127 Trieste, Italy

Received June 30, 1998; Revised Manuscript Received October 1, 1998

ABSTRACT: The thermoreversible gelation of syndiotactic poly(methyl methacrylate) in toluene has been investigated in detail. The two-step mechanism, proposed in an earlier publication, has been confirmed and illustrated in detail through the combination of FTIR investigations and rheological and NMR observations. The basic steps of this gelation mechanism are the equilibrium coil-to-single helix transition (first step) and the helix association into dimers (second steps) and larger multichain association units. The coil-to-helix transition is a true equilibrium process that can be detected separately through kinetic trapping. The comparative analysis of the infrared and rheological data and the temperature dependence of the line widths of the ^1H signals support the validity of this proposition.

Introduction

Syndiotactic poly(methyl methacrylate) (sPMMA) is able to form gels in many solvents and its gelation has been extensively studied in the past using different techniques.^{1–7} In a previous paper,⁸ a two-step mechanism for such a thermoreversible gelation in toluene was proposed. The experimental data suggested as the first step an intramolecular coil to helix transition. Association of these helices in a second step leads to the formation of a physical network. The process showed an important hysteresis between cooling and heating experiments. Such a hysteresis was tentatively ascribed to the difference in stability between the (single) helix and the associated structure.

This process of gelation has been further investigated in more detail using Fourier transform infrared (FTIR) spectroscopy, high-resolution ^1H nuclear magnetic resonance (NMR) spectroscopy, and rheology.

The change in molecular conformation as a function of time and temperature is followed by FTIR. The trans-gauche (TG) monomer conformation is characteristic of the random coil conformation of the polymer chain. In the helix, a monomer conformation close to the all-trans (called the TT conformation) dominates: it gives rise to a specific absorption band centered at 860 cm^{-1} .⁹ This band will be called the “conformational band” and results from the $-\text{CH}_2-$ rocking vibration.

The effect of temperature and time on the molecular mobility in the polymer solutions will result in a change in the ^1H spectral line width.

Rheological observation will provide information on the kinetics of network formation and on the viscoelastic properties of the resulting networks.

Experimental Section

Materials. sPMMA was polymerized in toluene in different ways. sPMMA samples 1–3 were polymerized using alumi-

num triethyl and titanium(IV) chloride as the catalyst (ZN) at different temperatures. sPMMA-4 was polymerized anionically (A) with sodium naphthalene as initiator. The characteristics of the polymers are reported in Table 1.

Methyl methacrylate (Aldrich, reagent p.a.) and toluene (Aldrich, reagent p.a.) were dried with calcium hydride and distilled under high vacuum for further purification.

The polymer concentration is expressed as polymer mass fraction, w_2 . The experimental investigations were performed on solutions having $w_2 = 0.10$.

Experimental Techniques. FTIR experiments were performed with a Perkin-Elmer FTIR-2000 infrared spectrophotometer. A sealed liquid MIR-ATR cell was used, and the temperature was controlled through the use of a thermostated circulating liquid. Dynamic observations were made at a scanning rate of $0.7\text{ }^\circ\text{C}/\text{min}$. No subtraction of the spectrum of the solvent was performed because shifts in the spectrum of the solvent can occur as a consequence of the possible interaction of the solvent with the polymer. The use of an internal reference was not necessary, as the concentration was kept constant for all the measurements performed in the reflection mode.

High-resolution NMR experiments were performed by means of a Bruker AC 200 spectrometer equipped with a multinuclear 5 mm probe.

Rheological observations were performed with a Rheometrics ARES rheometer, equipped with parallel plate geometry, at controlled temperatures, using an external circulation thermostat.

Results and Discussion

FTIR Observations. (a) Temperature-Dependent Observations. A representative spectrum of the polymer solution at $20\text{ }^\circ\text{C}$ is given in Figure 1. The change of the intensity of the conformational band of sPMMA-1 in a toluene solution was followed during a cooling–heating experiment. The observed intensities at 860 cm^{-1} are plotted as a function of temperature in Figure 2. At elevated temperatures, the intensity is

Table 1. Characteristics of the sPMMA Samples

sample	polymerization temp, °C	$10^{-3}M_n$	$10^{-3}M_w$	M_w/M_n	% syndiotactic triads	% heterotactic triads	% isotactic triads
SPMMA-1	-78 (ZN)	120	157	1.31	88.8	11.2	0.0
SPMMA-2	-56 (ZN)	53	96	1.81	77.3	16.8	5.9
SPMMA-3	-45 (ZN)	155	259	1.67	74.2	20.1	5.7
SPMMA-4	-73 (A)	256	376	1.46	77.0	21.4	1.4

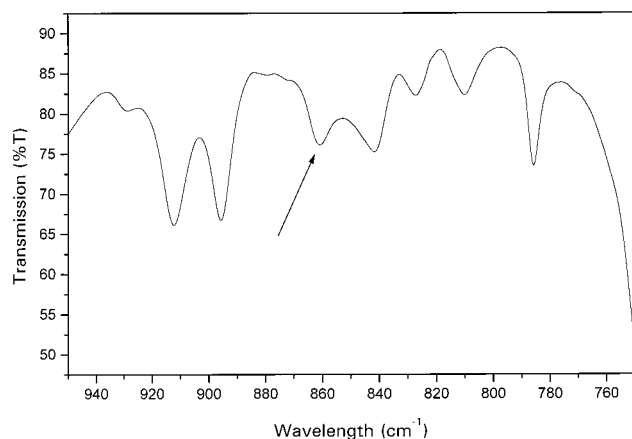


Figure 1. Representative infrared spectrum of sPMMA-2 in toluene $w_2 = 0.1$ at 20 °C. The conformational band is indicated by the arrow.

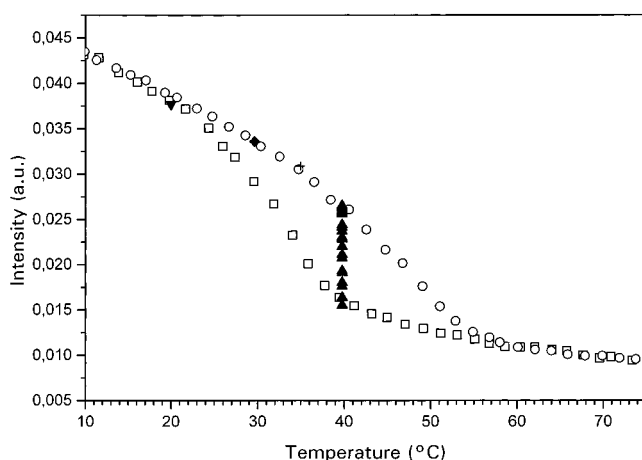


Figure 2. Intensity of the conformational band as a function of temperature and time: cooling (\square); heating (\circ); equilibrium values after isothermal annealing at 20 °C (\blacktriangledown), 29.7 °C (\blacklozenge), and 35 °C ($+$). Increase of the intensity during isothermal annealing at 39.8 °C (\blacktriangle).

very low and the polymer is predominantly in the random coil or TG conformation. The spectrum is similar to the one obtained at room temperature in a good solvent like chloroform. A slight increase of the intensity with decreasing temperature is observed in the high-temperature region. A deviation from an almost perfect linear trend sets in below 55 °C and the increase of intensity with decreasing temperature follows an S-shaped curve. The behavior becomes again linear below 20 °C. An important hysteresis is observed on heating, and the linear behavior is again reached around 58 °C.

This intensity–temperature relation strongly depends on the overall degree of syndiotacticity and, therefore, on the synthetic procedure by which this tacticity was realized. The curves obtained with different samples are represented in Figure 3A–D. A lower degree of syndiotacticity results in a reduction of the overall degree of transformation, a broadening of the transition

on the temperature scale, and a shift to lower temperatures. An albeit similar degree of tacticity, however obtained through either anionic or Ziegler–Natta polymerization, also leads to a strongly different behavior (compare Figure 3D,B). Almost no change in intensity is observed with the anionically prepared sample, and no gel is formed. The Ziegler–Natta sample on the contrary clearly shows the transition in conformation and the formation of a gel. Although no quantitative information on the exact stereotactic monomer distribution is known, it is clear that the different polymerization procedures lead to polymer chains with different distributions of stereoregular units along the chains and therefore to different average lengths of syndiotactic sequence. This can be estimated from the difference in heterotactic and isotactic triad content at constant fraction of syndiotactic triads. A larger number of heterotactic triads is characteristic for a larger number of transitions between stereoregular sequences (cf. Table 1). Anionic polymerization is therefore expected to result in the most random distribution and the shortest average regular sequence length.

(b) Isothermal Investigations. The change of the intensity of the conformational band was followed as a function of time at constant temperature for sPMMA-1. The samples were quenched in the FTIR cell from 80 °C to a predetermined temperature between 45 and 20 °C, and the increase with time of the intensity of the conformational band at that temperature was followed. The measurements were started when the given annealing temperature was reached after rapid cooling. The change of intensity with time is represented in Figure 4 for various temperatures.

At all temperature values, a plateau value is eventually reached. The time needed to reach this value increases with increasing temperature. At the lowest temperatures the plateau is reached very rapidly, indicating that most of the intensity increase has developed already in the cooling process, as fast as the latter may be. This behavior is known to take place in the case of reversible conformational transitions of biopolymers close to the midpoint temperature (T_m). At higher temperatures the transformation is much slower, and it can easily be followed as a function of time. This intensity increase at 40 °C is represented in Figure 2.

The plateau value, further called the “equilibrium value”, represents the maximum degree of transformation from coil to helix that can be reached at every temperature. The corresponding intensity–temperature curve will be called the “equilibrium curve”. These values coincide with the intensity values measured during a heating experiment (Figure 2).

(c) Hysteresis on Heating. From Figure 2 it is clear that a sample that is heated from below 20 °C to above 60 °C will show an important hysteresis because of the undercooling needed to induce structural transformations. The hysteresis can be partially or even completely suppressed in two slightly different ways and this will be illustrated for the sPMMA-1 sample. The common feature of the two methods is the presence of a (very

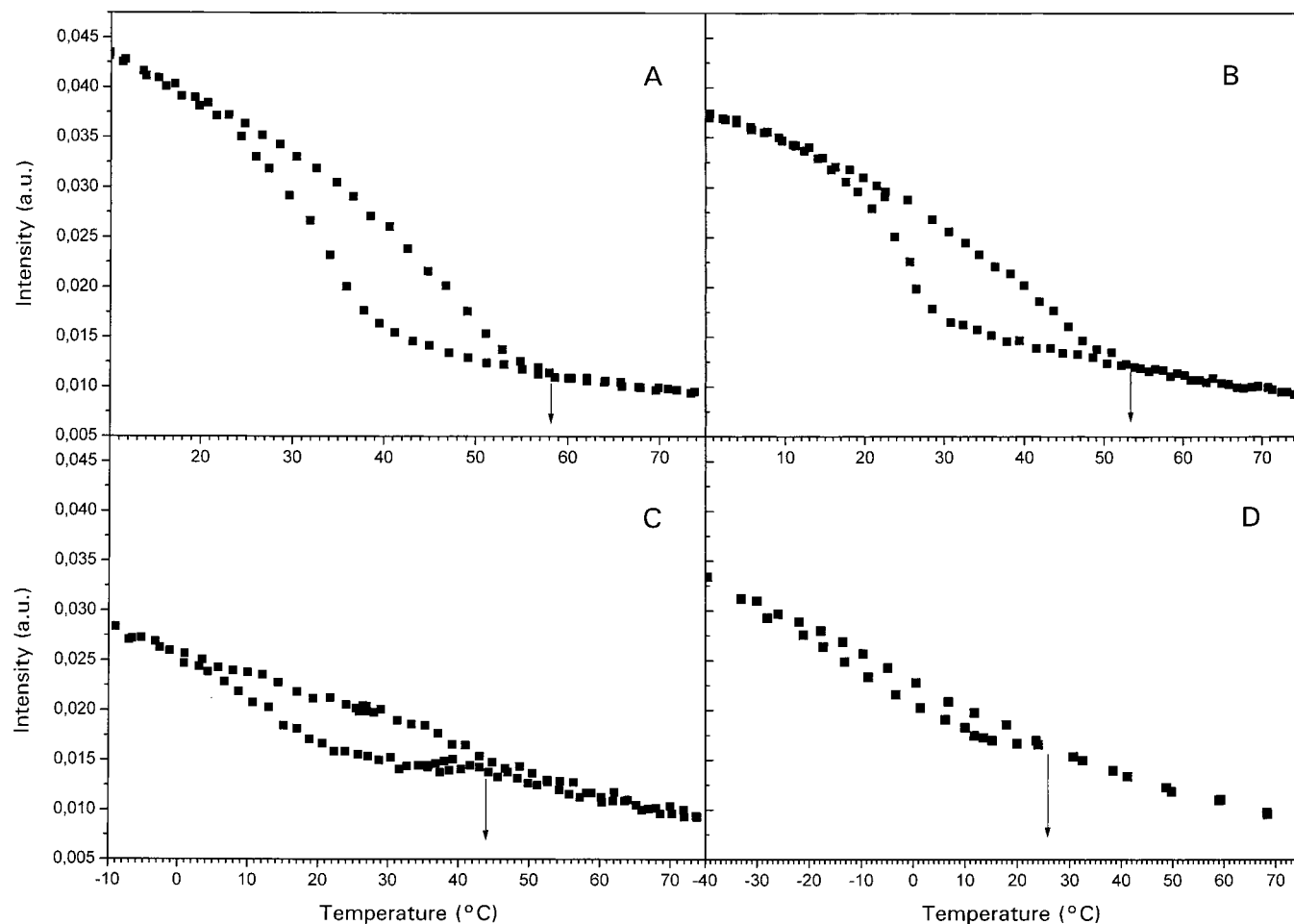


Figure 3. Influence of the tacticity on the intensity–temperature relationship of the conformational band: (A) sPMMA-2; (B) sPMMA-3; (C) sPMMA-4; (D) sPMMA-5. An arrow indicates the end melting point.

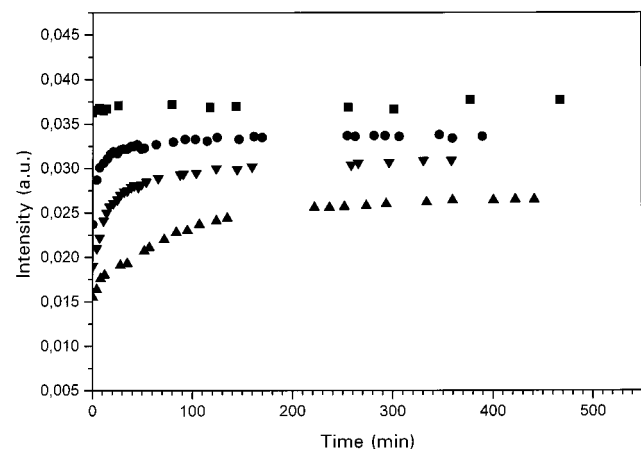


Figure 4. Intensity of the conformational band as a function of time at different temperatures: 20 °C (■); 29.7 °C (●); 35 °C (▼); 39.8 °C (▲).

similar) critical temperature above which hysteresis will be present anyhow.

The first way is to limit the heating of the sample in such a “dynamic” experiment only up to about 35 °C. As long as this temperature is not exceeded, any temperature change (i.e., either heating or cooling) will correspondingly move the intensity along the “equilibrium curve”. However, when this temperature is exceeded, hysteresis will set in and become more pronounced the higher the temperature to which the sample has been heated.

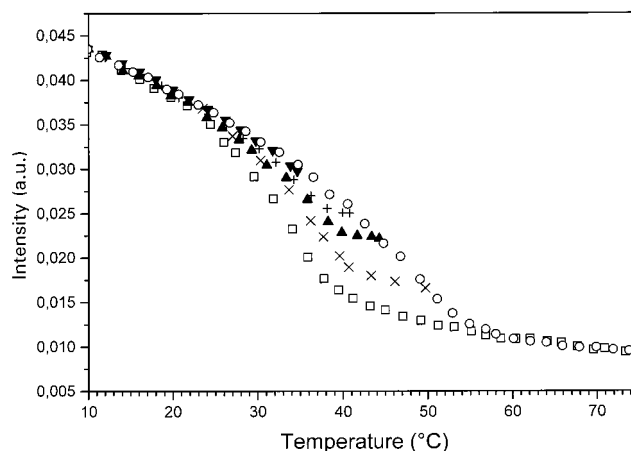


Figure 5. Relation between the temperature at which the sample is heated and the extent of hysteresis on cooling. Cooling (□) and heating (○) curve as in Figure 2. Cooling after heating to 35 °C (▼), 40 °C (+), 45 °C (▲) and 50 °C (×).

The data represented in Figure 5 were obtained in the following way. The sample was first cooled from 80 to 10 °C. This results in the same cooling curve as the one represented in Figure 2. Then, in separate experiments, the sample was heated to 50, 45, 40, and 35 °C, respectively. Every time the sample was again cooled to 10 °C. The temperature limit for the absence of hysteresis is situated around the temperature at which a more significant increase in intensity is observed on cooling.

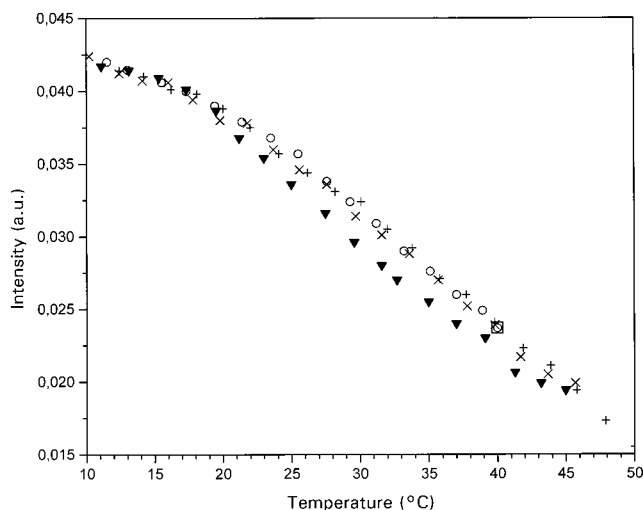


Figure 6. Cooling and heating experiment after isothermal annealing. Plateau value after isothermal annealing at 40 °C (\square). Cooling after isothermal annealing (\circ). Subsequent heating to 45 °C (\times). Cooling after heating to 45 °C (∇) and final heating curve ($+$).

Hysteresis can be suppressed also by *isothermal annealing* of the sample. This is illustrated in Figure 6 for an annealing temperature of 40 °C for 7 h. Once the "equilibrium curve" is reached, cooling and heating without exceeding 40 °C will proceed without hysteresis in the intensity–temperature relationship. When the sample is heated to higher temperatures (e.g., 45 °C), hysteresis is again observed.

(d) Influence of Annealing Time. In the previous series experiments, annealing times of the order of hours have to be used to reach the "equilibrium values". When this annealing is extended over periods of days, no further change in the "equilibrium value" at the different annealing temperatures is anymore observed. The thermal stability, however, increases, and this increase is more pronounced as the annealing temperature is increased. The melting domain becomes narrower. Annealing in the high-temperature region results in an increase of the final melting point. This is illustrated in Figure 7.

Conformational Change and Rheological Observations. (a) Temperature-Dependent Observations. A sample was subjected to the same temperature cycle as the one applied in the "dynamic" FTIR observations. The change of G' was followed, and the observed values are reported in Figure 8 as a function of temperature. The change in FTIR intensity is also reported in this figure. The raw experimental data have been corrected for the nonhorizontal linear dependence in the high-temperature region and rescaled to ensure an easier possibility of comparison with the G' data. The steep increase in G' sets in at a significantly lower temperature than the corresponding increase in intensity of the conformational band. On heating, a parallel decrease is observed up to around 35 °C. Then G' increases while the intensity of the conformational band continues to decrease. This increase produces a maximum, since it is followed by a steep decrease toward higher temperatures.

(b) Isothermal Experiments. The rheological data on isothermal annealing, presented in a previous paper⁸ were reexamined in view of the data obtained during this research. They are represented in Figure 9, together with the corresponding intensity changes of the

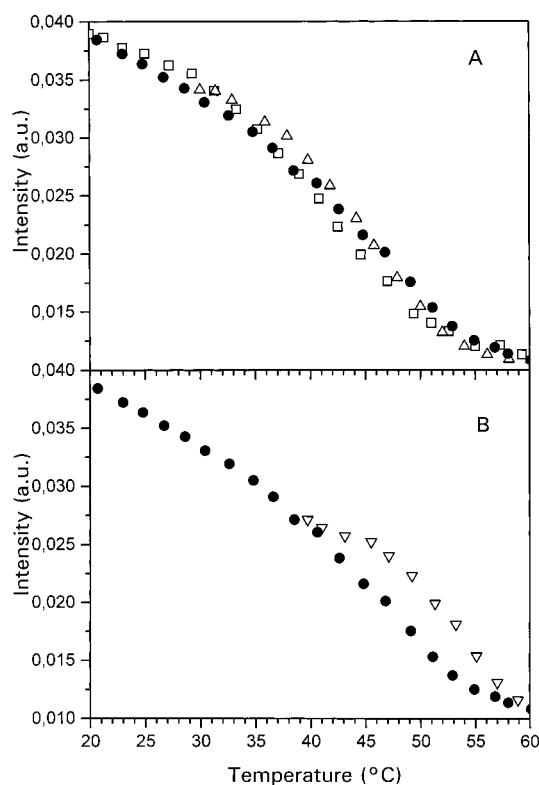


Figure 7. Influence of long time annealing on the stability of the formed structures. Heating (\bullet) curve as in Figure 2. (A) Heating after isothermal annealing for 7 days at 20 °C (\square) and 30 °C (\triangle). (B) Heating after isothermal annealing for 7 days at 40 °C (∇).

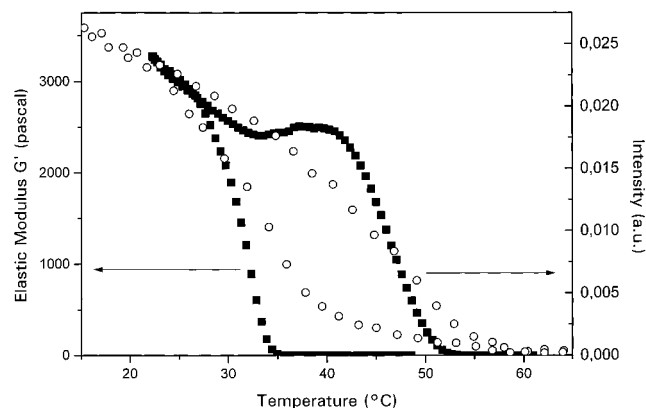


Figure 8. Intensity of the conformational band (\circ) and the elastic modulus (\blacksquare) as a function of temperature.

conformational band and the temperature profile used in these experiments.

The solution is initially cooled to 40 °C and kept at this temperature for a few hours. This produces an "equilibrium value". Parallel with this change in helicity with time, an increase of the elastic part of the modulus, G' , to a plateau value is realized. Then the sample was heated to 46 °C. This results in a decrease of the modulus and the helicity along the "equilibrium curve" to a new plateau value, following exactly the temperature–time profile. Cooling to 20 °C results in an increase of these two properties, again following very well the temperature–time profile. Heating a second time to 46 °C brings the sample back to the same situation as in the first heating. The sample turns into the isotropic liquid state above 60 °C.

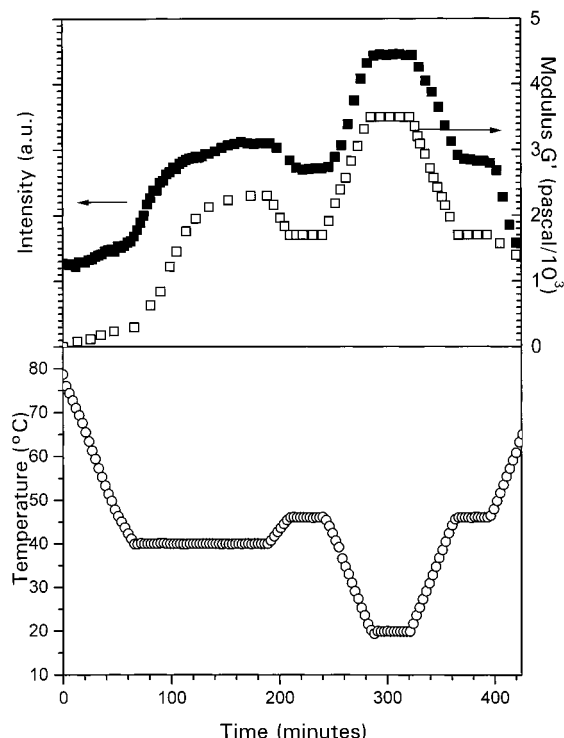


Figure 9. Combined FTIR and rheological experiment of sPMMA-1 in toluene: temperature (○); intensity (■); dynamic modulus G' (□).

NMR Observations. (a) Theoretical Considerations. The influence of temperature on molecular mobility can be studied through the evolution of the ¹H spectral line width (lw). This line width is directly related to the transverse relaxation rate, R_2 , which in turn depends on the correlation time (τ_c) of the overall reorientation tumbling:

$$lw = \nu_{1/2} \cong 1/\pi T_2$$

$$R_2 = T_2^{-1}$$

Since for macromolecular systems τ_c is very long, it is possible to simplify the mathematical form of the spectral density function $J(\omega, \tau_c)$. As a sound first approximation, an Arrhenius dependence of τ_c from temperature, T , can be assumed, providing that the weighted average of the internuclear distances does not significantly change upon changing temperature.

$$\tau_c^{-1} = k \exp(-\Delta G^\ddagger/RT) \quad (1)$$

Under these assumption all such geometrical contributions are collectively grouped in a preexponential term, k , independent of T . As a result, an exponential dependence of R_2 from T^{-1} is expected, as reported in eq 2:

$$R_2 = k \exp(\Delta G^\ddagger/RT) \quad (2)$$

Operationally, the line width can be reported as a function of T , according to eq 2:

$$\ln(\nu_{1/2}) = K + (\Delta G^\ddagger/R)T^{-1} \quad (3)$$

ΔG^\ddagger is the activation free energy for the overall tumbling motion. As a consequence, a polymer in a

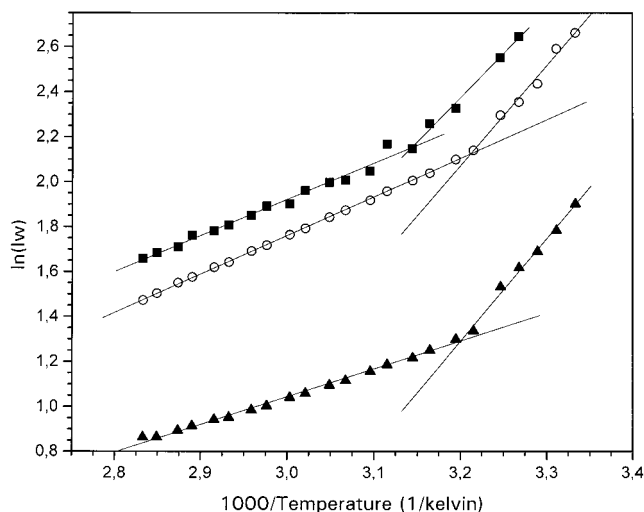


Figure 10. Line width as a function of temperature: CH_2 (■); CH_3 (○); OCH_3 (▲).

given, constant conformation should exhibit a linear plot of $\ln(\nu_{1/2})$ versus T^{-1} in which the slope is proportional to $\Delta G^\ddagger/R$. When a sudden structural or conformational variation occurs, *two* linear regions are observed. In this paper only the transition temperatures, marking the transition from one to the other conformation, will be reported.

(b) Experimental Observations. The line width was followed as a function of temperature at a cooling rate similar to the one used in the FTIR experiments. Their natural logarithm values were plotted as a function of T^{-1} in Figure 10.

Two linear regions can easily be recognized in this figure for the methylene-chain backbone units, the α -methyl group, and the ester methyl group. They are separated by a well-defined transition temperature, T_{conf} . At this temperature, a reduction of the mobility of these groups occurs, implying an important increase of the activation free energy. The values of T_{conf} are different for the main chain $-\text{CH}_2-$ units (45.5 °C) and the α - CH_3- and ester $-\text{CH}_3-$ groups (38.5 °C).

Discussion

The data presented in this paper support the two-step mechanism already proposed in a previous publication. An equilibrium coil-to-helix transition precedes the intermolecular association that leads to the physical network formation. This conclusion is based on the following observations:

- Hysteresis is absent when a sample that has been cooled in a dynamic experiment to 10 °C is heated to a temperature that does not exceed 35 °C. Subsequent heating and cooling between these two temperature limits will move the sample along the "equilibrium" intensity-temperature curve.

- Isothermal annealing will result in a maximum value of coil-to-helix transformation at every temperature, and this intensity is situated on the intensity-temperature curve obtained on heating. Once this "equilibrium curve" is reached, subsequent cooling and heating between the annealing temperature and, e.g., 10 °C will move the system along this curve without any hysteresis. Heating above the annealing temperature will restore the hysteresis that will become more pronounced as the annealing temperature is higher. The value of G' changes parallel with this change in conformation.

•Annealing times longer than those necessary to reach the “equilibrium value” will not change the degree of coil-to-helix transformation but will increase the stability of the structures formed and reduce the width of the transition region. The intensity decrease on heating in the high-temperature region can only proceed at higher temperatures.

•The important change of G' with temperature on cooling will take place at a lower temperature than the change in intensity of the conformational band. The change of G' with time and temperature in the high-temperature region follows exactly the intensity changes observed in FTIR. Once the “equilibrium value” is reached, hysteresis is also absent in the G' -temperature behavior.

•The NMR data indicate that the change in mobility of the main chain sets in around the temperature at which the first deviation from the linear decrease of the intensity of the conformational band is observed. A change of the mobility of the side methyl groups sets in at a lower temperature. The participation of the solvent in this process of chain stiffening is possible. Such a solvent participation was already proposed in the literature.¹⁰

From these observations a complex mechanism can be proposed to account for the temperature-induced gelation of sPMMA in toluene.

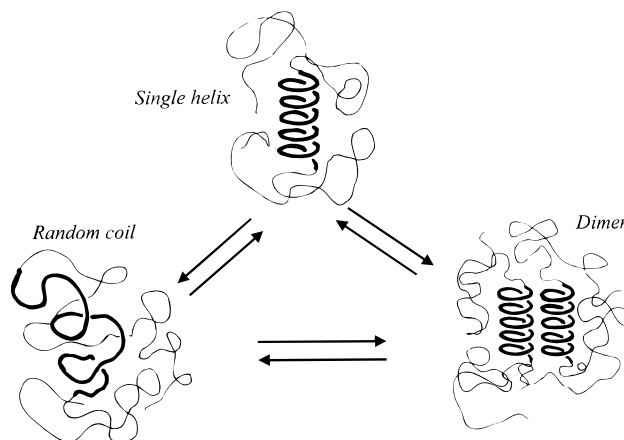
The conceptual “ingredients” of such a mechanism are (i) the equilibrium conformational and molecular entities which prevail, or coexist, depending on system conditions; (ii) the thermodynamics of the conformational transition and interchain association; and (iii) the kinetics of the interconversion between the different conformational entities.

As far as point i is concerned, stretches of the polymer chains of still unknown length (“cooperative unit”) are postulated to interconvert between the following conformational elements: a disordered or coiled conformation (“c”), associated with a low value of the IR band at 860 cm^{-1} and a TG monomer conformational sequence; the fundamental ordered conformation, which can reasonably be identified with the already proposed single helix (“h”), associated with a high value of the IR band at 860 cm^{-1} and the TT conformational sequence; the basic interchain association unit, i.e., an ordered dimer (“d”), which differs from “h” only as to the molecularity—i.e. 2 versus 1—but shares with it the same high value of the IR band at 860 cm^{-1} and the TT conformational sequence. Obviously, only additional direct evidence of structural nature could shed some light onto the topology of this dimer, e.g., being a “side-by-side” dimer or an intertwined double helix.

Eventually, upon increasing the polymer concentration, after a further decrease of temperature and possibly after some annealing, larger multichain association units (“m”) can be formed, with a molecularity higher than 2, as the result of the extensive association of several conformationally ordered elements “h” and/or “d”. However, for mere reasons of simplicity, in the following description only the three basic conformational entities will be considered, i.e., “c”, “h”, and “d”, the formation of the multichain “m” units being considered just a kinetically more hindered extension of the “d” ones.

From the thermodynamic standpoint, it follows that the equilibria to be considered in a first approximation are: “c” \rightleftharpoons “h”, “c” \rightleftharpoons “d”, “h” \rightleftharpoons “d”. The last one

Scheme 1. Simplistic Representation of the Multiple Equilibria between the Random Coil, Single Helix and Dimer Conformation



obviously does not imply any additional change of the IR absorption at 860 cm^{-1} . The multiple equilibria are simplistically sketched in Scheme 1.

The rheological findings reported in Figure 8 (heating part of the cycle, considered as “equilibrium values”) clearly indicate that, upon heating, the disruption of an ordered structural component (the “h” one) contributing to the overall rigidity (as manifested by G') of the network takes place at lower temperatures, largely transforming into another ordered one, with an even larger value of G' , as indicated by the maximum of the $G'(T)$ function.

In molecular terms and due to the observed temporary increase of rigidity, the latter structure must be related to “junctions” in the gel, i.e., the “d” ones. It is then forceful to conclude that the transition from helix to coil proceeds at a lower temperature than the transition from dimer to coil. Formally, it implies that the (equilibrium) thermodynamic stability of the dimeric structures persists to higher temperatures than that of the helical ones [$G'_{\text{dimer}}(T) < G'_{\text{helix}}(T) < G'_{\text{coil}}(T)$]. This evidence finds a counterpart in the observed shift to higher temperatures of the equilibrium curve after long-time annealing, shown in Figure 7b.

However, a very interesting but complicating feature comes out of the kinetic behavior of the conformational transition/gelation process.

Upon cooling, a hysteresis appears in the formation of the ordered conformation, as monitored by the development of the TT-related IR band (see Figures 2 and 3). Such a hysteresis effect could either merely reflect an unspecific delay in the development of the ordered junction elements or, alternatively, be related to the unveiling of a different underlying true equilibrium, namely “c” \rightleftharpoons “h”. The validity of the latter hypothesis is confirmed by the comparative analysis of the IR(T) and $G'(T)$ cooling curves of Figure 8a as well by the NMR data of Figure 10. The former set of results clearly indicates that conformational ordering (from IR) takes place much earlier (upon lowering T) than the setup of a significant formation of junctions (from G'). Roughly, about one-third of the maximum extent of ordering, as calculated at about 15°C , is already formed when the G' curve just starts to rise steeply at about 34°C .

In parallel, the line widths of the ^1H signals (see Figure 10) depart from the high- T linear behavior well before the G' upraise. This break indicates the onset

of an extra stiffening of the main chain (for CH_2 protons: starting at 45.5°C), followed by the side groups ($\alpha\text{-CH}_3$ and ester CH_3 protons: starting at 38.5°C), which altogether must be related to the TG to TT conformational change and lead to the coil-to-helix transition of the polymer repeating units. It is the obvious kinetic prerequisite to the further pairing of the ordered stretches producing the "dimers" and the related dramatic increase of G' . Such combined evidence indicates that at a scan rate typical of these investigations (about $0.7^\circ\text{C min}^{-1}$) the first step of the mechanism of gel formation is the transition from coil to helix. This is a kinetically controlled process, because, as has already been shown, the helical dimer is in principle thermodynamically more stable in that temperature range (e.g., from about 55 to about 35°C). However, the " c " \rightleftharpoons " h " is a really true equilibrium, while the possibility of separate detection may be looked upon only through a kinetically trapping, thanks to the comparatively fast cooling process.

The second step is the intermolecular association of helices through dimerization (and eventually through further multimerization), leading to physical cross-linking and to the gelation of the solution. Of course, the possibility of formation of a negligible amount of dimers at high temperature in such a dynamic experiment cannot be excluded. However, if present, it would only manifest as an increase of G' —that is, viscosity—and not as the large extent required by the thermodynamic conditions.

All that would correspond to a high energetic barrier for the "coil-to-dimer" transition, certainly much larger than the sum of those involved in the sequential steps "coil-to-helix" and "helix-to-dimer", despite the already assessed order of thermodynamic stability [$G^\circ_{\text{dimer}}(T) < G^\circ_{\text{helix}}(T) < G^\circ_{\text{coil}}(T)$]. This situation, both regarding the thermodynamic stability of the various forms and the corresponding activation energy profiles, is represented in Figure 11.

Only the " h " \rightleftharpoons " d " equilibrium prevails in the low-temperature range, devoid of the complications due to the presence of the kinetically biased disorder-to-order transformations. This easily explains the absence of hysteresis in that range of T , where any interconversion benefits from an already substantial population of helices, which are the kinetically controlling elements of the process of chain pairing. However, with increasing temperature the fraction of helical segments decreases more rapidly than the fraction of dimers. Any recooling starting in the higher temperature region would then be accompanied by the reappearance of hysteresis, which will be more marked the higher the temperature.

The above model seems to be self-consistent and able to explain all the experimental observation. Obviously,

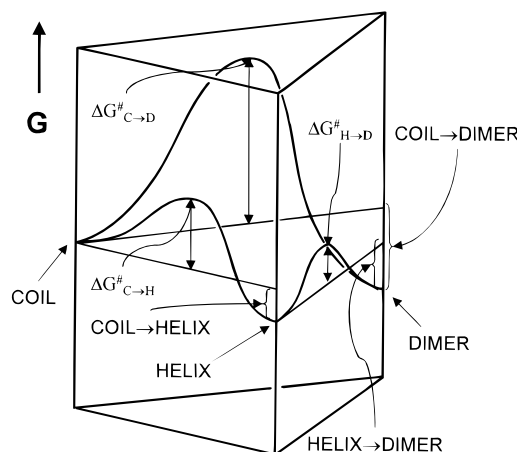


Figure 11. Energy diagram with corresponding activation energies for different conformational transitions. It is clear from the figure that $\Delta G^\ddagger_{C \rightarrow D} \gg \Delta G^\ddagger_{C \rightarrow H} > \Delta G^\ddagger_{H \rightarrow D}$. $\Delta G^\ddagger_{x \rightarrow y}$: activation energy for transition from conformation x to conformation y , with C = random coil, H = single helix, and D = dimer.

more information is to be collected on the system, possibly including studies in different solvents. Moreover, it should be brought to attention that the possibility of a delicate interplay of kinetics and of thermodynamics in shaping the complex phase behavior of polymeric systems has been convincingly addressed in another recent publication.¹¹

Acknowledgment. The authors thank Ms. E. Leon for technical assistance. The authors also are indebted to the Fund for Scientific Research Flandres, the IUAP IV/P4-11 for financial support and to the University of Trieste.

References and Notes

- (1) Berghmans, H.; Donkers, A.; Frenay, L.; Stoks, W.; De Schryver, F. C.; Moldenaers, P.; Mewis, J. *Polymer* **1987**, *28*, 97.
- (2) Spevacek, J.; Schneider, B. *Adv. Colloid Interface Sci.* **1987**, *27*, 81.
- (3) Spevacek, J.; Schneider, B. *Polym. Bull.* **1980**, *2*, 227.
- (4) Spevacek, J.; Schneider, B.; Straka, J. *Macromolecules* **1990**, *23*, 3042.
- (5) Mrkvickova, L.; Stejskal, J.; Spevacek, J.; Horska, J.; Quadrat O. *Polymer* **1983**, *24*, 700.
- (6) Spevacek, J.; Suchoparek, M. *Macromolecules* **1997**, *30*, 2178.
- (7) Saiani, A.; Spevacek, J.; Guenet, J.-M. *Macromolecules* **1998**, *31*, 703.
- (8) Berghmans, M.; Thijs, S.; Cornette, M.; Berghmans, H.; De Schryver, F. C.; Moldenaers, P.; Mewis, J. *Macromolecules* **1994**, *27*, 7669.
- (9) Dybal, J.; Stokr, J.; Schneider, B. *Polymer* **1983**, *24*, 971.
- (10) Kusuyama, H.; Miyamoto, N.; Chatani, Y.; Tadokoro, H. *Polym. Commun.* **1983**, *24*, 119.
- (11) Keller, A., et al. *Macromol. Symp.* **1997**, *124*, 67.

MA981017T